

# Optimization of Porosity Response in Electroless Ni-YSZ Co-Deposition

Nor Bahiyah Baba\*, C. W. Mastura, C. W. MdZin, Nurul Hazwani Ghazemi, and Siti Nor Azuani AbdLahli

Faculty of Manufacturing Engineering Technology, TATI University College, Kijal, Kemaman, Terengganu, Malaysia; bahiyah@tatiuc.edu.my, cwmastura@gmail.com, wanie\_achik@gmail.com, ctazuani@yahoo.com

## Abstract

**Background/Objectives:** The paper discusses on the porosity content optimization by varying electroless nickel co-deposition process parameters in the Ni-YSZ coating. **Methods/Statistical Analysis:** The Ni-YSZ co-deposition was produced by electroless nickel process co-deposited with 8mol% Yttria Stabilized Zirconia (YSZ) powder on alumina substrate. Electroless Nickel (EN) process parameters investigated in the study were bath loading ranges between 225-150 ml, bath temperature ranges 84-94oC, stirring speed between 250-500 rpm and pore formers namely graphite, activated carbon and starch. Design of Experiment (DoE) Taguchi L9 method was used and analyzed by statistical tool analysis of variance (ANOVA) in Minitab software. **Findings:** The rank of parameters affecting the porosity response is the bath loading, poreformer, stirring speed and lastly the bath temperature. The best optimum condition at nominal setting for porosity response is bath loading at 225 ml, bath temperature at 89oC and stirring speed at 375 rpm. Graphite pore former gives the most reliable porosity formation compared to activated carbon and starch. This was supported by the Scanning Electron Microscope (SEM) micrographs. **Applications/Improvements:** In general, standard bath temperature of 89oC and moderate stirring speed at 375 rpm that gives better porosity content. Coating surface was analyzed using SEM coupled with Energy Dispersive X-ray (EDX) which shows the presence of nickel and YSZ elements.

**Keywords:** Activated Carbon, Electroless Nickel, Graphite, Pore Former, Porosity, Starch, YSZ

## 1. Introduction

Nickel ceramic composites are well known for its outstanding properties and applications. Its applications include corrosion, thermal and also wear resistance<sup>1,2</sup>. Nickel ceramic coating can be produced by many ways such as thermal and chemical deposition. One of the chemical deposition methods is electroless coating. The electroless coating method was developed by Brenner and Riddell in the middle of the twentieth century<sup>3</sup>. This method requires no electricity in the coating process. It is a chemical reduction process, which depends on the catalytic reduction of a metallic ion from an aqueous solution which contain the reducing agent and the subsequent deposition of the metal<sup>4</sup>. The reducing agent

in electroless nickel solution is oxidized and Ni<sup>2+</sup> ions are deposited onto the substrate surface as Ni metal and the first layer of deposited Ni acts as a catalyst for the continuous process<sup>5</sup>. This electroless nickel coating is one of the excellent technique and widely used in order to gain good properties of ceramic composite coating such as uniform coating thickness, electrical conductivity and also high corrosion resistance<sup>6</sup> while porous Nickel-Yttria-Stabilized Zirconia (Ni-YSZ) showed reasonable electrical conductivity at 800<sup>o</sup>C, reasonable ionic conductivity and high thermal resistance<sup>7,8</sup>.

Porous ceramic materials have been used in various applications such as ceramic filters and membranes, fuel cell electrodes and also thermally insulating bulk materials<sup>9-12</sup>. The properties of porous ceramics rely upon

\* Author for correspondence

its morphology, size and distribution of pores and the level of interconnection between them which describe the permeability, the density and also thermo-mechanical properties<sup>13-15</sup>. The pore forming agent has the great potential to tend high porosity levels. There are reports that numerous pore forming agent have been investigated include starch<sup>16-18</sup>, graphite<sup>19,20</sup>, Propylene (PP) and Polymethylmethacrylate (PMMA)<sup>21</sup>. Li et al. reported the incorporation of starch pore forming increased the porosity with the starch amount lower than 30 vol%<sup>22</sup> and Novais et al. find that PMMA and PP open high porosity level after burn out<sup>21</sup>. Essentially, the organic particles are burnt out to the firing temperature then leave the voids in the ceramic body. The void's morphology depends on the selected type of pore former which then could be controlled by the appropriate incorporation content and particle size distribution<sup>21</sup>.

Electroless Nickel coating provides a range of corrosion protection from good to excellent depending on the process selected. Coating thickness, substrate condition and surface preparation procedures are also important factor which determines both coating porosity and the ultimate resistance to corrosive attack. Studies showed that certain porosity level in the deposition is critical as the amount of porosity enhanced thermal insulation for thermal barrier coatings and gas circulation in fuel cell anode<sup>22,23</sup> applications. Adequate amount of porosity required is in the range of 30-40%. It is found that the amount of porosity in the coating should not exceed 40 vol.% as the greater amount reduces the mechanical properties of the deposit. Thus, an adequate amount of porosity and reasonable mechanical properties should be balance. Studies found that the amount of porosity in Electroless Nickel deposition could be induced by varying the agitation methods, deposition rate, bath pH, substrate surface condition and incorporate pore former. Archimedes specific density can be used to measure the porosity fraction in a material. The basic Archimedes principle states that the amount of displaced water volume is equal to the immersed object volume. The determination of the solid substance density can be done by buoyancy or displacement methods<sup>24</sup>.

There are many Electroless Nickel process parameters that can affect the amount of porosity in the Ni-YSZ co-deposition. Analyzing and solving a multiple performance characteristics is a challenging research problem which is time consuming and exorbitant in cost. Statistical Design of Experiments (DoE) Taguchi's method uses a special design of Orthogonal Array (OA) to analyze the optimal

condition resulting in valid and objective conclusions<sup>25</sup>. There are four parameters to investigate namely bath loading, bath temperature, stirring speed and pore former types at 3 levels.

## 2. Experimental Work

Electroless Nickel co-deposition is an autocatalytic process. The addition of ceramic YSZ particles in the bath will cause a co-deposition of metallic nickel and ceramic YSZ onto the substrate. The details on the methodology was described in previous study<sup>26</sup>. In order to enhance the amount of Ni-YSZ composite coating, several EN process parameters were chosen as listed in Table 1. In this study, EN process parameters such as bath loading, bath temperature, stirring speed and incorporation of pore former were investigated for high quantity and quality surface coating.

**Table 1.** Experimental EN process parameters

Parameters	Level		
	1	2	3
Bath loading /ml	150	180	225
Bath temperature/°C	84	89	94
Stirring speed/rpm	250	375	500
Pore former	Graphite	Activated carbon	Starch

## 3. Results and Discussion

### 3.1 Design of Experiment

The Taguchi L9 Orthogonal Array DoE response was analyzed using a statistical tool analysis of variance (ANOVA) in Minitab 15. The advantage of Taguchi DoE is it is robust, cost and time saving to determine the optimum process parameters. The effect of EN process parameters on the porosity content in the coating was investigated based on 95% confidence level.

Minitab 15 analyzed the porosity response against all the four parameters at 3 levels. The main effect plot for means porosity response is shown in Figure 1. Comparing the means data of all four parameters, it is found that bath loading gives the largest effect of approximately 0.18. This indicates bath loading is the major parameter affecting the porosity response. Followed closely is the pore former (0.12), then the stirring speed (0.04) and lastly the bath temperature with 0.02 effects. The rank of parameters effect on porosity response is bath loading, poreformer, stirring speed and lastly the bath temperature.

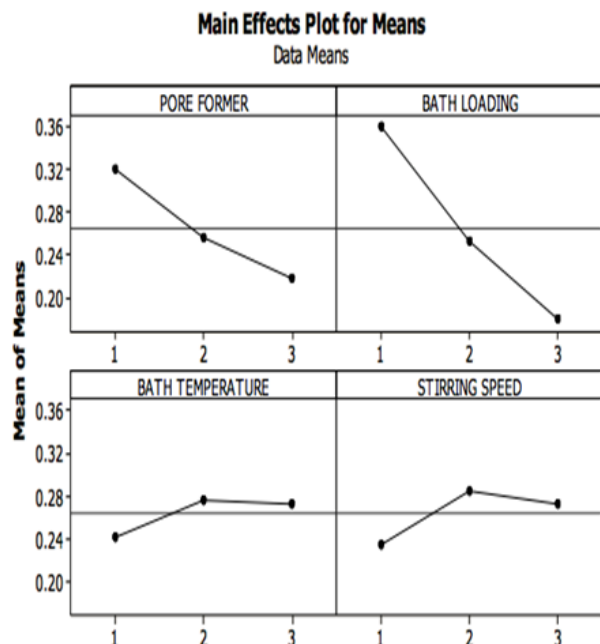


Figure 1. Main effect plot for the porosity response.

Signal to noise ratio was set to nominal is the best. The porosity response is aimed to achieve not more than 40 vol.%. This is so because allowing more than 40 vol.% porosity in the coating will cause lower mechanical properties. The porosity response measurement was obtained in a range of 10 to 65 vol.%. Thus, nominal is the appropriate target.

The main effects plot for SN ratios is shown in Figure 2. The most significant effect was the bath loading parameter at level 3. The next in line is the bath temperature at level 2 and followed closely is the stirring speed at level 2. The pore former SN ratio effect is almost negligible or insignificant as the variance is very close to nominal line. Hence, the best optimum condition for porosity response is bath loading at 225 ml, bath temperature at 89°C and stirring speed at 375 rpm. The effect of pore former is insignificant, thus it can be excluded.

Considering both effect for means and SN ratio, it can be concluded that bath loading the major contributor to have a good amount of porosity within the coating. Bath loading is the amount of YSZ particles pour into the bath. Overall, the optimum condition for Electroless Ni-YSZ co-deposition process parameter on porosity are bath loading at 225 ml, bath temperature at 89°C and stirring speed at 375 rpm.

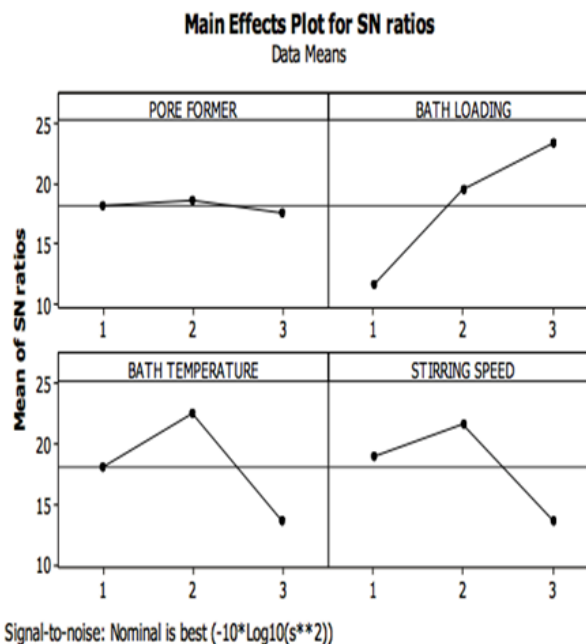


Figure 2. Plot graph SN ratio versus pore former, bath loading, bath temperature and stirring speed.

### 3.2 Effect of EN Process Parameters on Porosity Response

An analysis on the effect of bath loading ranges between 150-225 ml on the porosity response was conducted. The variation of bath loading for a different type of pore former is given in Figure 3. The targeted porosity content in the coating is approximately 40 vol.%. It was found that the highest porosity obtained was 55.01% at 150ml bath loading for graphite pore former. It is shown that low bath loading deposited high porosity content. Besides, the graphite pore former is an excellent pore forming agent which produces high porosity to the ceramic as reported by Niiet al<sup>27</sup>. In general, it shows that graphite and activated carbon pore formers give acceptable porosity contents. On the other hand, starch gives a very poor performance of all. Upon heating, most of starch sample are flaking instead of evaporating. This indicates that the starch was not burned out during heating.

Another varying parameter studied is the effect of bath temperature which are 84 C, 89 C and 94 C for three types of pore former. The EN Slotonip suggest 89°C as the optimum bath temperature, but this is for optimum Ni deposition alone. In this experiment, Ni will be co-deposited with YSZ ceramic particle as well as the addition

of pore former. Figure 3 shows the variation of porosity content with bath temperature for different types of pore former. It was found that the performance of porosity content trend depends on the types of pore former. All types of pore former performed well at temperature 89°C. This means the EN bath optimum temperature also applied to EN-YSZ co-deposition.

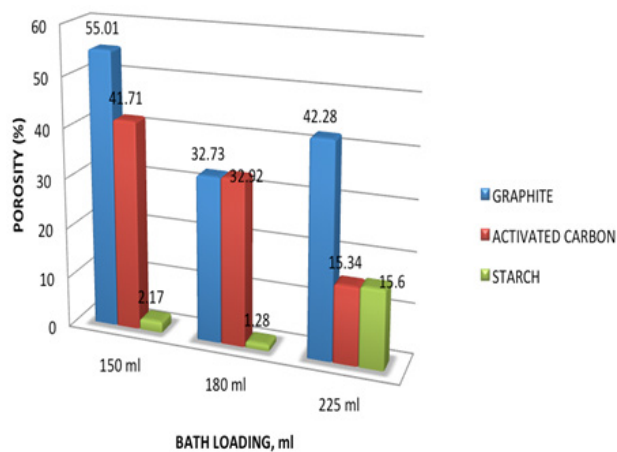


Figure 3. Porosity versus pore former for various bath loadings.

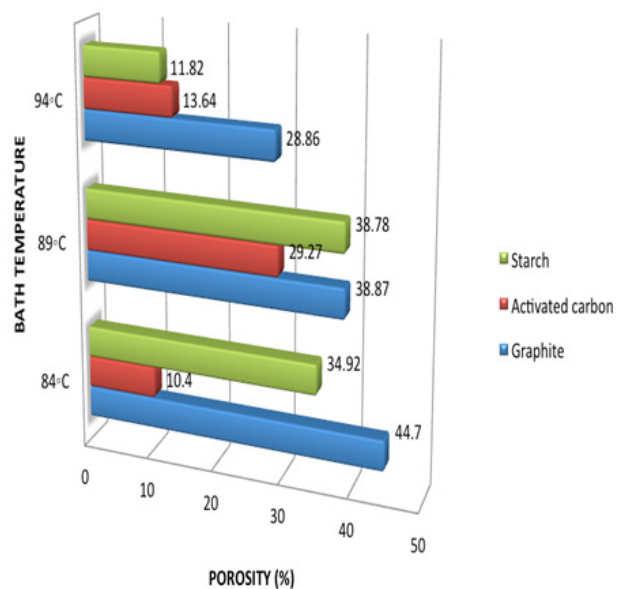


Figure 4. Porosity versus bath temperature for various pores former.

The effect of bath agitation stirring speed of 250rpm, 375 rpm and 500 rpm on the porosity content is also analyzed. The variation was conducted in 3 groups of

different types of pore former. The highest porosity contained obtained is 65.32% as showing in Figure 5 at 375 rpm for starch pore former. The porosity content is higher than targeted. It was found that most of the starch pore former samples were cracked and flaking out. This might be the main reason for high porosity measurement.

General trend showed in Figure 4 is the porosity content of Ni-YSZ co-deposition increased to maximum value at 375 rpm stirring speed except for activated carbon pore former which the highest porosity obtained at 225 rpm. As for activated carbon, it is the carbonaceous agent that has some excellent properties such as low density, large surface area, chemical stability and fast adsorption kinetics<sup>28</sup>. Thus, this explained for obtaining the maximum porosity content at a high level of stirring speed. Since the targeted porosity is 40 vol.%, a way to control the deposition of activated carbon should be investigated.

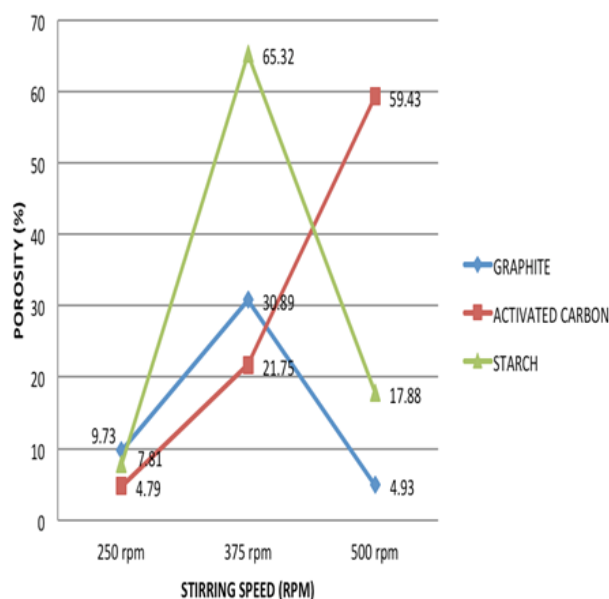
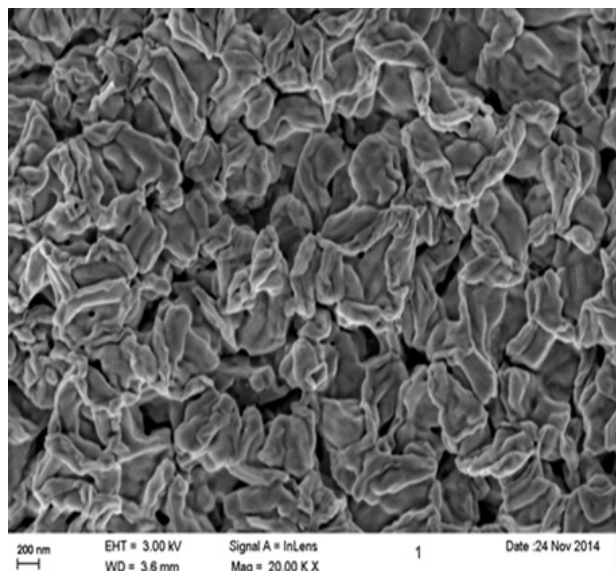


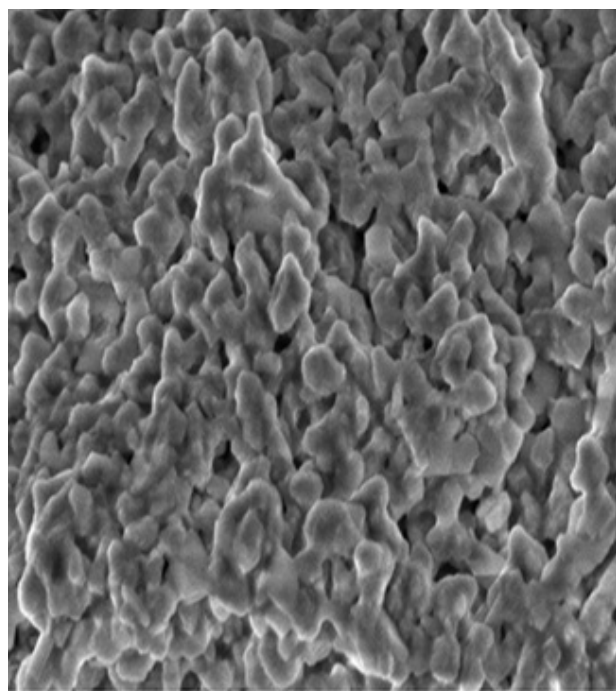
Figure 5. Porosity versus stirring speed for various pore former.

### 3.3 SEM Micrograph and EDX Spectrum

The surface of Ni-YSZ co-deposition coating was analyzed using Scanning Electron Microscope (SEM) couple with Energy Dispersive X-ray (EDX) analysis. The purpose of the SEM-EDX analysis is to determine the structures of porosity on the ceramic coating by analyzing the micrograph as well as the elemental analysis obtained.

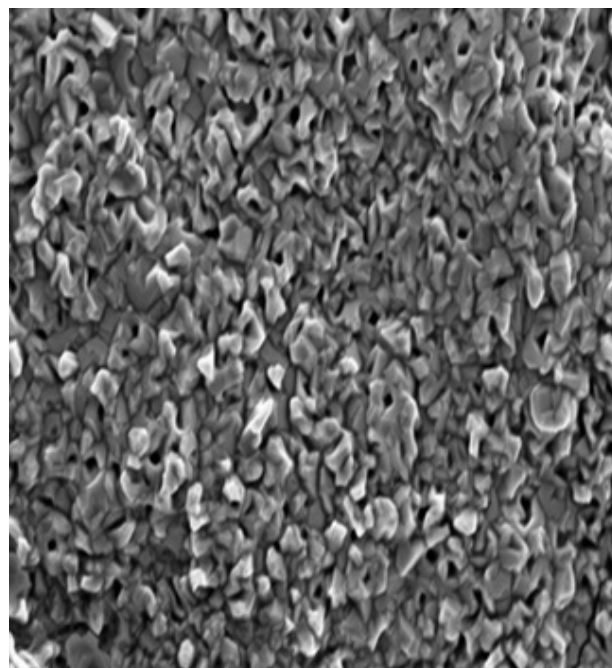


(a)



(b)

that distinct grain morphologies and pores can be seen in these figures.



(c)

**Figure 6.** SEM micrographs of (a) graphite (b) activated carbon and (c) starch.

These micrographs of Ni-YSZ co-deposition coating was captured after the removal of pore former by heating to 700°C for one hour. In Figure 6, it can be seen that the shape and type of porosity formed significantly depends on the type of pore forming agent. Graphite and activated carbon pore formers in Figure 6(a) and 6(b) showed similarity where the porosity seemed to have interaction underneath the upper surface. The microstructure is overlapped and staggered show the possibility for more porosity underneath the upper surface.

Comparing these two to the starch pore former in Figure 6(c), the porosity seemed to be more superficial. It looks like the microstructure is clog underneath the first surface. Visually, the microstructure of graphite and activated carbon are less dense compared to the starch pore former.

Figure 7 illustrates the EDX spectrum using both of Energy Dispersed X-ray micro-analyzer (EDX) and SEM shows the major peaks of Zirconium (Zr), Nickel (Ni), Carbon (C) and Oxygen (O). These confirmed that the composites were composed of combination of metallic nickel and ceramic YSZ.

Ni-YSZ co-deposition coating samples at the optimum condition for the porosity response of bath loading 225 ml, bath temperature 89°C and stirring speed 375 rpm were chosen for each pore former. The SEM micrographs show the image of porosity on the coating samples. Figure 6 is the SEM images for different type of pore formers such as graphite, activated carbon and starch at 20 kX magnification and 200 nm scale. It is apparent

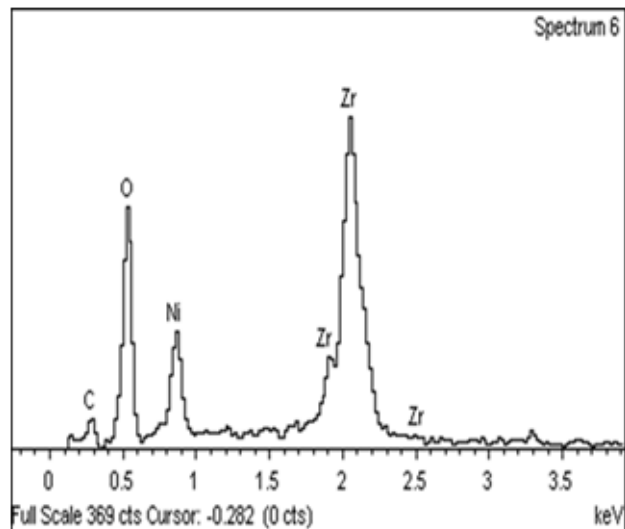


**Figure 7.** EDX spectrum of Ni-YSZ co-deposition coating.

## 4. Conclusions

The effect of EN process parameters on the Ni-YSZ co-deposition porosity content was investigated. There are four EN process parameters chosen namely bath loading, bath temperature, stirring speed and types of pore former. The effect of bath loading, bath temperature and stirring speed on porosity varied depending on the types of pore former. The types of pore former were not highly affecting the formation of high porosity within the coating. It is shown that low bath loading deposited high porosity content. All types of pore former performed well at temperature 89°C. This means the EN bath optimum temperature also applied to EN-YSZ co-deposition. The porosity content of Ni-YSZ co-deposition increased to a maximum value at 375 rpm stirring speed except for activated carbon pore former. The rank of parameters affecting porosity response is bath loading, pore former, stirring speed and lastly the bath temperature. Whereas, the best optimum condition for porosity response at nominal setting is bath loading at 225 ml, bath temperature at 89°C and stirring speed at 375 rpm. The SEM micrographs compared the microstructure of varying types pore former where the graphite and activated carbon pore former give better porosity network compared to the starch pore former. The EDX spectrum confirms the presence of Ni-YSZ major peaks.

## 5. Acknowledgment

The author would like to express her gratitude to Kementerian Pendidikan Malaysia for their financial support in Fundamental Research Grant Scheme (FRGS) on the research titled “The Fundamental Study of Electronics Nickel Co-Deposition Process for Higher Porosity and Ceramics Particle Incorporation”.

## 6. References

1. Kundu S, Das SK, Sahoo P. Properties of electroless nickel at elevated temperature A review. *Procedia Engineering*. 2014; 97:1698–706.
2. Gengler JJ, Muratore C, Roy AK, Hu J, Voevodin AA, Roy S, Gord JR. Ytria-Stabilized Zirconia-based composites with adaptive thermal conductivity. *Composites Science and Technology*. 2010 Nov; 70(14):2117–22.
3. Brenner A, Riddell GE. Nickel plating by chemical reduction. *Nature*. 1948 Jul; 162. p. 183–4.
4. Balaraju JN, Narayanan TS, Seshadri SK. Electroless Ni–P composite coatings. *Journal of Applied Electrochemistry*. 2003; 33(9):807–16.
5. Khosroshahi NB, Khosroshahi RA, Mousavian RT, Brabazon D. Effect of electroless coating parameters and ceramic particle size on fabrication of a uniform Ni–P coating on SiC particles. *Ceramics International*. 2014 Sep; 40(8):12149–59.
6. Farzaneh A, Mohammadi M, Ehteshamzadeh M, Mohammadi F. Electrochemical and structural properties of electroless Ni–P–SiC nanocomposite coatings. *Applied Surface Science*. 2013 Jul; 276:697–704.
7. Baba NB, Davidson A. Investigation of Ni-YSZ SOFC anode fabricated via Electroless Nickel co-deposition. *Procedia Engineering*. 2011; 23:474–8.
8. Davarpanah A, Yaremchenko AA, Fagg DP, Frade JR. Ni-YSZ cermet for solid oxide fuel cell anodes via two-step firing. *International Journal of Hydrogen Energy*. 2014 Sep; 39(27):15046–56.
9. She J, Ohji T, Deng ZY. Thermal shock behavior of porous silicon carbide ceramics. *Journal of the American Ceramic Society*. 2002 Aug; 85(8):2125–7.
10. Tsuru T. Inorganic porous membranes for liquid phase separation. *Separation and Purification Reviews*. 2001; 30(2):191–220.
11. Muhammed GS. Efficiency enhancement of crystalline silicon solar cell by the deposition of undoped ZnO thin film. *Indian Journal of Science and Technology*. 2011 Jun; 4(6):677–80.
12. Gregorova E, Pabst W. Porous ceramics prepared using poppy seed as a pore-forming agent. *Ceramics International*. 2007 Sep; 33(7):1385–8.

13. Colombo P. Engineering porosity in polymer-derived ceramics. *Journal of the European Ceramic Society*. 2008; 28(7):1389–95.
14. Tang F, Fudouzi H, Uchikoshi T, Sakka Y. Preparation of porous materials with controlled pore size and porosity. *Journal of the European Ceramic Society*. 2004; 24(2):341–4.
15. Paiva AEM, Sepulveda P, Pandolfelli VC. Processing and thermomechanical evaluation of fibre-reinforced alumina filters. *Journal of Materials Science*. 1999 Jun; 34(11):2641–9.
16. Zivcova-Vlckova Z, Locs J, Keuper M, Sedlarova I, Chmelickova M. Microstructural comparison of porous oxide ceramics from the system  $\text{Al}_2\text{O}_3$ - $\text{ZrO}_2$  prepared with starch as a pore-forming agent. *Journal of the European Ceramic Society*. 2012 Aug; 32(10):2163–72.
17. Khattab RM, Wahsh MM, Khalil NM. Preparation and characterization of porous alumina ceramics through starch consolidation casting technique. *Ceramics International*. 2012 Aug; 38(6):4723–8.
18. Garrido LB, Albano MP, Genova LA, Plucknett KP. Influence of starch type on characteristics of porous 3Y- $\text{ZrO}_2$  prepared from a direct consolidation casting method. *Materials Research*. 2011 Jan-Mar; 14(1):39–45.
19. Sarikaya A, Dogan F. Effect of various pore formers on the microstructural development of tape-cast porous ceramics. *Ceramics International*. 2013 Jan; 39(1):403–13.
20. Sanson A, Pinasco P, Roncari E. Influence of pore formers on slurry composition and microstructure of tape cast supporting anodes for SOFCs. *Journal of the European Ceramic Society*. 2008; 28(6):1221–6.
21. Novais RM, Seabra MP, Labrincha JA. Ceramic tiles with controlled porosity and low thermal conductivity by using pore-forming agents. *Ceramics International*. 2014 Sep; 40(8):11637–48.
22. Li S, Wang CA, Zhou J. Effect of starch addition on microstructure and properties of highly porous alumina ceramics. *Ceramics International*. 2013 Dec; 39(8):8833–9.
23. Wang L, Wang Y, Sun XG, He JQ, Pan ZY, Zhou Y, Wu PL. Influence of pores on the thermal insulation behavior of thermal barrier coatings prepared by atmospheric plasma spray. *Materials and Design*. 2011 Jan; 32(1):36–47.
24. Baba NB. YSZ Reinforced Ni-P composite by Electroless Nickel co-deposition. Hu N, Rijeka, Croatia. *European:IN-TECH Open Access Publisher*;2012.
25. Simwonis D, Thulen H, Dias FJ, Naoumidis A, Stover D. Properties of Ni/YSZ porous cermet for SOFC anode substrates prepared by tape casting and coat-mix® process. *Journal of Materials Processing Technology*. 1999 Aug; 92-93:107–11.
26. Baba NB, Lahli SNA. Physical studies on Electroless Ni-YSZ composite coating. *ARPN Journal of Engineering and Applied Sciences*. 2015 Sep; 10(17):7825–9.
27. Nie L, Liu J, Zhang Y, Liu M. Effects of pore formers on microstructure and performance of cathode membranes for solid oxide fuel cells. *Journal of Power Sources*. 2011 Dec; 196(23):9975–9.
28. Zubizarreta L, Arenillas A, Pis JJ. Carbon materials for  $\text{H}_2$  storage. *International Journal of Hydrogen Energy*. 2009 May; 34(10):4575–81.